Food Packaging and Shelf Life 30 (2021) 100759

Contents lists available at ScienceDirect

Food Packaging and Shelf Life

journal homepage: www.elsevier.com/locate/fpsl

Effect of plasma treatment on improving liquid retention capacity of capillary recesses for food packaging applications

Alaa Alaizoki [a,*], Christopher Phillips [a], David Parker [b], Craig Hardwick [b], Chris Griffiths [c], Davide Deganello [a,*]

[a] Welsh Centre for Printing and Coating, College of Engineering, Swansea University, Bay Campus, Fabian Way, Swansea, SA1 8EN, UK
[b] Klockner Pentaplast, Wakefield Road, Featherstone, West Yorkshire, WF7 5DE, UK
[c] SPECIFIC IKC, Swansea University, Central Avenue, Port Talbot, SA12 7AX, UK

ARTICLE INFO

Keywords:
PET
Oxygen plasma
Wettability
Capillary valves
Meat exudate

ABSTRACT

Liquid residue is a major issue in fresh food packaging, especially for meat products. This work investigates capillary recesses directly integrated into PET packaging film, with targeted plasma treatment of the recesses to enhance their liquid retention capacity. Localised oxygen plasma treatment (oxygen flow rate: 80 cm^3/min, pressure: 0.14 mbar, power: 240 W) of PET recesses introduced polar oxygen groups onto their surface and increased their wettability. It is proposed that the difference in wetting characteristics of the recesses and rest of the packaging surface enhanced the capillary valve effect, which dramatically increased the liquid retention capacity. Untreated recess samples (diameter: 9 mm) had retention capacity of around 0.70 g, which increased to 1.50 g after localised O_2 plasma treatment. Even after aging of over 60 days, the plasma-treated recesses maintained the enhanced retention capabilities. The estimated resulting retention capacity of recesses of diameter 9 mm was 2972 ± 62 mL/m^2, which is comparable with conventional absorbent pads (3000 mL/m^2). This demonstrated the viability of applying plasma treatment in food packaging to effectively isolate any excessive exudate using only the packaging film.

1. Introduction

Food packaging has a vital role in prolonging food shelf life and ensuring safer and fresher food in the supply chain (Biji et al., 2015). However, excessive liquid residues and moisture within the packaging is still a big challenge to fresh food packaging, in particular for liquid-exuding food, such as meat, fish and poultry (Gaikwad et al., 2019). These food products are mostly packaged in plastic trays and tend to release an exudate (drip) during refrigerated storage (Gouvêa et al., 2016). The meat exudate is an aqueous juice primarily composed of soluble sarcoplasmic proteins (Kim et al., 2013). It flows under gravity from the meat surface due to protein denaturation and lateral shrinking of muscle fibres during the post-mortem period. The exudate expressed from fresh meat is estimated around 1–3 % wt. of the meat cut weight and it can reach 10 % wt. for pale-soft, exudative (PSE) meat (Huff-Lonergan & Lonergan, 2005). The exudate lost also increases during meat handling or processing, such as cutting and freezing (Warner, 2017). High exudate content has a negative impact on the food packaging as it accelerates quality deterioration and compromises safety of the packaged food. This is due to the increase in water activity, which enhances the growth of spoilage microorganisms and pathogenic bacteria (Gaikwad et al., 2019; Gouvêa et al., 2016). Further, the accumulated exudate on the bottom of packaging trays is prone to leakage during handling and displaying in the market, and perceived unattractive by customers (Gouvêa et al., 2016). Therefore, it is crucial to isolate the free-moving exudate in food packaging.

Various techniques have been developed to isolate the liquid exuded in food packaging including absorbent meat pads (Baldwin et al., 2007; Realini & Marcos, 2014; Schmidt, 2013) and polymeric foam trays with open-cell structure (Han, 2009; Maga et al., 2019). However, additional components such as absorbent pads and foams present a problem in terms of recycling of the packaging film since soaked pads and foams are non-recyclable, and these are often glued to the packaging and must be manually removed (Durdag et al., 2014; Jensen & Versteylen, 2008; Licciardello, 2017). Further, food trays with integrated micro-capillary features to act as a soak-away is an alternative solution used for

* Corresponding authors.
E-mail addresses: 972353@swansea.ac.uk (A. Alaizoki), d.deganello@swansea.ac.uk (D. Deganello).

https://doi.org/10.1016/j.fpsl.2021.100759
Received 13 April 2021; Received in revised form 7 September 2021; Accepted 26 September 2021
Available online 5 October 2021
2214-2894/© 2021 The Authors. Published by Elsevier Ltd. This is an open access article under the CC BY license (http://creativecommons.org/licenses/by/4.0/).

retaining the food exudate (Davidson et al., 2013). These capillary features have small sizes and suffer with other absorbent packaging solutions from limited absorption capacity (Davidson et al., 2013; LaRue et al., 2011; Otoni et al., 2016).

Capillary wetting (capillary phenomenon) is fundamentally based on capillary forces, which defines the spreading of a wetting liquid on a solid surface even against gravity (Si et al., 2018). Liquid in open capillary systems is commonly controlled by introducing capillary burst valves on their capillary channels (Zimmermann et al., 2008). This includes geometrical valves with a sudden change in their dimensions or hydrophobic valves, which are based variation of surface wettability. The capillary valve has a pinning effect on the liquid meniscus generating a pressure barrier as the meniscus adapts to the change in valve geometry or surface wettability (Cho et al., 2007; Feng et al., 2003; Wang et al., 2013; Zimmermann et al., 2008). The valving functionality was also studied for liquid trapping in closed capillary systems such a closed tube during vertical orientation and inclination. The liquid tends to drain from the open end of relatively large tubes by air finger propagation called Taylor fingering phenomenon (Davies & Taylor, 1950; Extrand, 2017, 2018a; Kumar et al., 2018). However, liquid drainage can be prevented for sufficient pinning effect and stable meniscus on the tube opening acting as a capillary valve (Extrand, 2017; Wang et al., 2013). This mechanism can be extrapolated to the capillary recesses used to trap exudate in food packaging. Therefore, the pinning effect can be enhanced for larger capillary recesses within the food packaging tray to increase their retention of meat exudate, which is thus the subject of this article.

Wettability of the capillary wall surface has a considerable impact on capillary liquid retention (Lu et al., 2013). Plasma treatment is among the most highly utilised surface modification techniques for increasing solid surface wettability. It is flux of excited particles, ions, electrons, neutral species and UV radiation. The plasma can functionalise the treated surface with introduced polar groups, such as C—OH and C═O leading to an increase in its hydrophilicity and free energy (Shenton & Stevens, 2001; Vesel & Mozetic, 2017). It is environmentally safe, inexpensive, uniform and suitable for polymers with heat sensitivity (Lee, 2010; Lee et al., 2009; Zille et al., 2015). Plasma treatment is commonly used in polymeric food packaging for enhancing printability of substrates, packaging disinfection, improving sealing and gas barrier characteristics (Pankaj et al., 2014).

In this work, it is proposed the selective application of plasma treatment to internal walls of capillary recesses to improve their surface wettability and free energy. This can induce valve functionality based on surface wettability variation, thus it may improve stability of the liquid menisci and liquid retention capacity. Therefore, it is essential to investigate the liquid retention capacity of larger-sized recesses with improved wall wettability to develop a viable solution for isolation of meat exudate in packaging trays. PET polymer was used for its wide popularity in food packaging, especially in meat packaging trays (Maga et al., 2019; Nisticò, 2020). This work used a combined approach of varying both size and surface wettability of capillary recesses. This was carried out with thermoformed polyethylene terephthalate (PET) inserts with capillary recesses of different sizes as liquid absorbers. Oxygen plasma treatment was applied to the capillary recess surfaces to investigate the plasma effect on their liquid retention capacity. Simulant liquids were used to mimic the real meat exudate in the liquid retention tests.

2. Materials and methods

2.1. Materials

Amorphous polyethylene terephthalate (PET) sheets with thickness of 0.50 mm (Klockner Pentaplast Group, UK) were used to thermoform inserts with capillary recesses. Isopropyl alcohol (IPA) (Propan-2-ol ≥ 99.5 %, Fisher Scientific, UK) was used to clean the recess surfaces by dipping and rinsing the samples in IPA solvent. Sodium carboxymethyl cellulose (CMC) powder (Sigma Aldrich, UK) with a molecular weight (M_w) of 90,000 g.mol^{-1} was used with deionised (DI) water to prepare a liquid (CMC 1 % wt.) as a simulated meat exudate. 4-Hydroxy-4-methyl-2-pentanone (Sigma Aldrich- boiling point: 166°C, density: 0.931 g/mL, surface tension: 32.37 mN/m) with methylene blue dye (Sigma Aldrich) were used for volume measurement of recess cavities. Triton X-100 surfactant (Sigma Aldrich, UK) was used to prepare the simulant liquids with different surface tension values. Red azorubine colorant- E122 (FastColours LLP, UK) was used to dye the simulant liquids for retention tests.

2.2. Design and thermoforming of inserts with capillary recesses

The 3D model design of an insert with arrays of capillary recesses was generated by computer-aided design (CAD) SolidWorks software (Edition SP 4.0- 2016) (Leite et al., 2018). The recesses had truncated cone shape with internal depth of 6 mm, draft angle of 10°. The opening diameters of the recesses were in the range of (4−12 mm). The insert was configured with arrays of 6 even-spaced recesses of the same diameter as shown in Fig. 1. The mould designing and thermoforming process to produce PET replicates of the insert with capillary recesses were carried out in Klockner Pentaplast Company, UK.

2.3. Shape profile and volume of capillary recesses

The dimensions and shape profile of the formed PET recesses were determined by digital Smartzoom 5 microscopy (Zeiss, UK). Cross-sections of the recesses with nominal diameters of 7, 8, 9, 9.5, 10, 11 mm were scanned, and 2D images were taken at magnification of x270 to generate their shape profiles. A measurement tooling for dimensions in Smartzoom 5 software was used to measure wall thickness, opening diameter, depth and draft angle of each recess (Carey et al., 2018; Erdogan & Eksi, 2014). Cavity volume of the recesses was determined by measuring the mass of a liquid, with known density, occupying the recess spaces. A low surface tension liquid (4-Hydroxy-4-methyl-2-pentanone stained with methylene blue dye) was used to give a better levelling with the recess edges. The liquid volume was then calculated by its known density as it represented the volume of the corresponding recess cavity (Sahin & Sumnu, 2007).

2.4. Preparation of simulant liquids

Aqueous solutions of (CMC) 1 % wt. were used as simulant liquids for fresh meat exudate. CMC is commonly used as thickener for food products, and its aqueous solutions of low concentrations show Newtonian behaviour (Klimovič & Pekař, 2007; Miehle et al., 2021). The simulant liquids were prepared to reflect the rheological properties of meat exudate reported in literature (Den Hertog-Meischke et al., 1998; Farouk et al., 2012; Ursu et al., 2016), with a wide range of surface tensions. The liquids had three surface tension values of 72.6, 52.3 and 31.5 mN/m by adding a surfactant (Triton X-100) to the CMC 1 % wt. solutions. All the three liquids had similar density and shear viscosity of 1.002 ± 0.001 g/mL and 5.60 ± 1.34 mPa.s respectively. These physical and rheological characteristics were measured at temperature of 20°C. The density measurement was conducted by gravity pycnometer (Fisher Scientific UK Ltd) as described by (Guo et al., 2012). Surface tension of the simulant liquids was determined by pendant drop technique using (First Ten Angstroms FTA1000c) analyser (Berry et al., 2015). The shear viscosity was measured by rotary rheometry (Gemini HR nano Rheometer) equipped with parallel plates (diameter: 60 mm, gap: 400 μm) (Ursu et al., 2016). The simulant liquids were dyed with red azorubine colorant- E122 (FastColours LLP) to be distinguished during the liquid retention tests (Extrand, 2017).

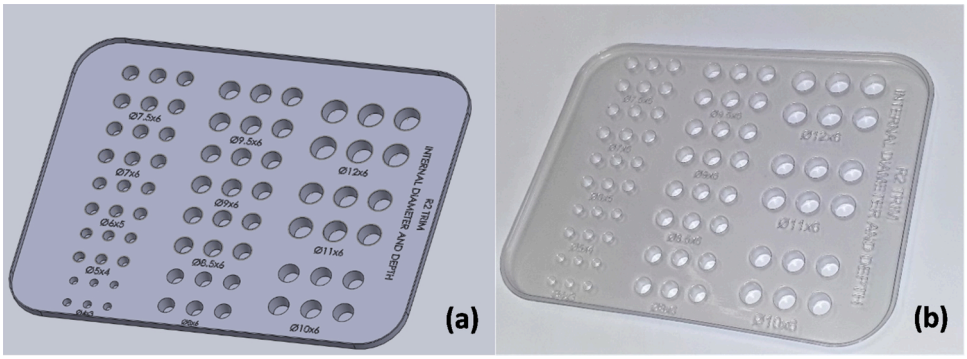

Fig. 1. (a) 3D model design, (b) photo of thermoformed PET test sample.

2.5. Oxygen plasma treatment of capillary recesses

The formed PET insert was trimmed to separate each 6-recess array of the same recess size in one sample. The recess samples were cleaned to eliminate any organic contaminants by rinsing with Isopropyl alcohol (Kostov et al., 2010). A low pressure plasma unit (model: Nano, Diener Electronic, Germany) with a cylindrical chamber (diameter: 26.7 cm, length: 42 cm) was used for the surface treatment. The plasma unit was coupled with a frequency generator sourced with 230 V AC supply to provide a power source at 40 kHz. The distance between the powered electrode and sample-holding tray was 15 cm. The glow discharge was produced by oxygen gas supply with the vacuum pressure (base pressure: 0.1 mbar) in the plasma chamber as modified via the gas flow rate. Based on application of plasma treatment, the recess samples were separated into groups (no treatment, localised plasma treatment of recess walls, plasma treatment of recess walls and edges) as illustrated in Fig. 2. The plasma treatments were carried out at oxygen flow rate of 80 cm^3/min, working pressure of 0.14 mbar and power of 240 W. The plasma settings (power, pressure, flow rate) were defined through preliminary testing on plasma treatment to consistently give targeted surface wettability of the PET samples, and in line with the equipment working range envelope. The recesses were treated for two exposure times of 6 and 18 s to obtain the target levels of surface hydrophilicity (Pandiyaraj et al., 2013; Xie et al., 2012). For localised plasma treatments of the recess walls, the selective plasma treatments of only internal surface of recess walls were conducted by placing an electrostatic film mask (made from polypropylene, PP) on the sample face surface as shown in Fig. S1 in the Supplementary material. The mask had holes for each recess, while it formed a barrier between PET surface and excited plasma species preventing the treatment of masked areas. The PP film mask was prepared via laser cutting (Epilog Laser) and discarded after the plasma treatment.

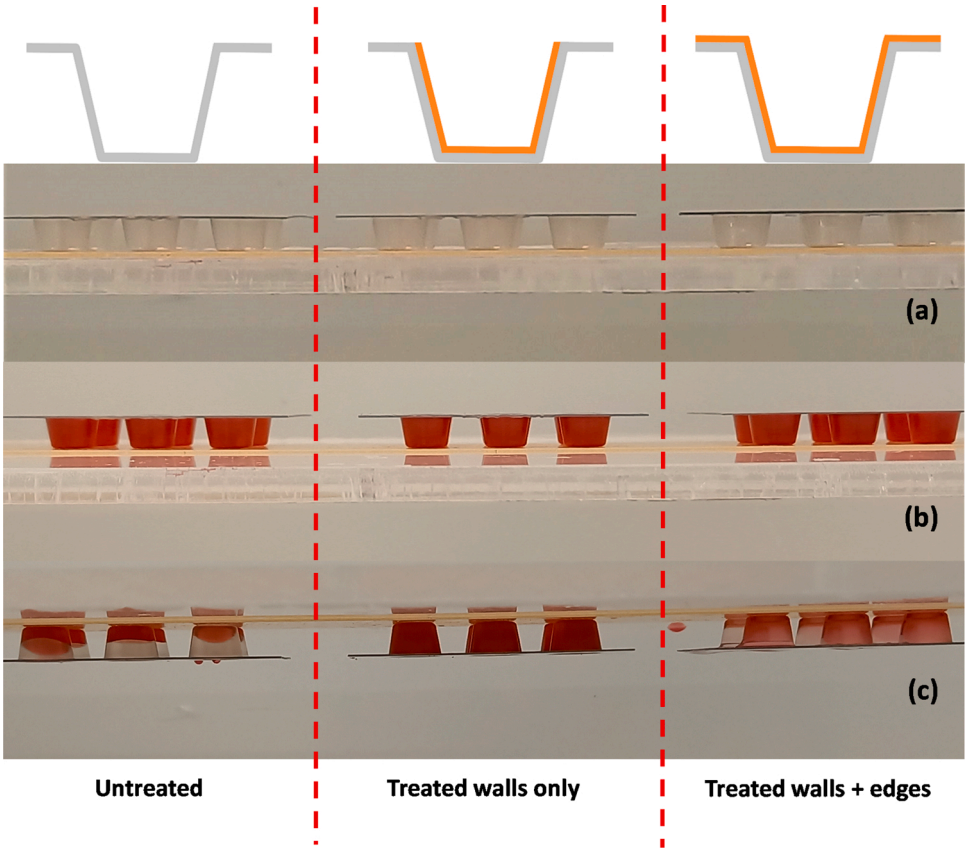

Fig. 2. Retention test with simulant liquid (CMC 1 %, γ: 72.6 mN/m) of PET recesses (untreated, plasma-treated walls, plasma-treated walls and edges) with nominal diameter of 10 mm; (a) empty recesses, (b) before tilting, (c) after tilting.

2.6. Characterisation of PET surface

2.6.1. Wettability and surface energy measurements

Static contact angle measurements were carried out by sessile drop technique to characterise the surface wettability of the PET recesses. The contact angle of 3 μL DI water drops was measured on flat surface of the untreated and plasma-treated recesses. The measurements were conducted in (First Ten Angstroms FTA1000c) analyser system at temperature of 20 ± 1°C and relative humidity of 54 ± 5 %. The contact angle values were obtained within 2 h after plasma treatment as a mean of measured values for 6 samples (Jucius et al., 2015). Surface energy (γ_s^{tot}) with the polar (γ_s^{p}) and dispersive (γ_s^{d}) components were also determined for the recess surfaces. The surface energy measurement was based on Owens-Wendt method using DI water and diiodomethane (Sigma Aldrich, 158429- 25 ML, UK) as polar and non-polar liquids with defined surface tension components respectively (Yang et al., 2009).

2.6.2. Surface chemical composition by X-ray photoelectron spectroscopy (XPS)

X-ray photoelectron spectroscopy (Kratos Analytical Ltd, UK) was used to analyse the surface chemistry of pristine and O_2 plasma-treated PET recess samples. The chemical composition of the PET surfaces was characterised (5 min after the plasma treatment) in the analysis chamber under pressure in order of 10^{-8} Torr. The sample surfaces were exposed to an exciting x-ray source of monochromatic Al Kα (1486.6 eV). The photoelectrons emitted from each analysis location area were analysed by hemispherical analyser. The charge effect of the polymer surfaces was neutralised by magnetic neutralisation lens. Each sample was scanned at pass energy of 160 eV in five analysis locations. The same analysis locations were also analysed with large area scan at pass energy of 20 eV. The resulting peaks were processed with CasaXPS software (Version 2.3.22PR1.0, Casa Software Ltd). The element peaks were fitted on Shirley background and calibrated according to the reference position of carbon C 1s peak of 285.0 eV (Dowling et al., 2012).

2.6.3. Surface topography by atomic force microscopy (AFM)

The effect of oxygen plasma on surface roughness of capillary recesses was evaluated by scanning their surface topography with atomic force microscopy (JPK NanoWizard 3). Cut samples in the size of 1 cm × 1 cm were taken from pristine and O_2 plasma-treated PET recesses and scanned by the AFM over areas of 1 μm × 1 μm in tapping mode as described by (Junkar et al., 2009). The scanning images were analysed by Gwyddion software (Version 2.55) to determine the surface roughness parameters. The roughness (Ra) and root mean squared roughness (RMS) values were averaged from scans of 3 different areas.

2.7. Liquid retention test of capillary recesses

Liquid retention capacity of the recesses was evaluated for various combinations of recess size and plasma treatment by retention test under normal gravity. The test included tilting the recess samples for an angle of 180° over 5 s, after filling with simulant liquids as shown in the Fig. 2. The weight of simulant liquid in full sample (6-recess array) was measured before tilting and mounted on a sticky tape on a built-in tilting board. The weight of trapped liquid in the tilted sample was then measured representing the liquid retention capacity (g) (Extrand, 2018a). The retention capacity was also estimated in mL/m^2 with simulant liquid (CMC 1 % wt., density: 1.002 g/mL) for recesses of optimised retention capacity. This was based on a hexagonal packing of recesses per square metre with spacing of 1 mm between the neighbouring recesses (Wardhani et al., 2014).

2.8. Ageing effect on plasma-treated capillary recesses

The effect of hydrophobic recovery on surface properties and liquid retention capacity of the plasma-treated recesses was assessed for different storage periods. The PET recess samples were treated with O_2 plasma for 18 s and stored in clean plastic boxes at controlled temperature of 20 ± 1°C (humidity 40–60 % RH). The degradation of wettability and surface energy was evaluated by measuring the contact angles of the test liquids on PET surfaces over storage times of 0, 1, 2, 3, 7, 14, 21, 28, 60 days. The chemical composition of the aged PET recess surfaces was analysed by XPS technique, and the liquid retention capacity was evaluated with CMC 1 % wt. (γ: 52.3 mN/m) under normal gravity (Homola et al., 2012).

3. Results

3.1. Shape profile and size of model and PET recesses

Geometrical characterisation of the PET recesses showed consistent wells in line with nominal dimensions. Detailed illustrations and data are presented in Supplementary material (Fig. S2 and Table S1). Fig. S2 shows cross-section profiles of recess model and thermoformed PET recess with diameter of 9 mm. All thickness, dimension and volume values were measured for recesses with nominal diameters (7, 8, 9, 9.5, 10, 11 mm) and presented in Table S1 in the Supplementary material. The PET recesses had a comparable replication of geometrical dimensions of their models with error less than 0.04 mm for opening diameters, 0.08 mm for depths and 3.17° for draft angles. The wall thickness profiles exhibited wall thinning towards the bottom corners. This is due to deformation and stretching during thermoforming process (Buntinx et al., 2014). The opening of the PET recesses had round corners due to irregular wall thickness resulting in a variation of their opening diameters. Therefore, the bottom of the round corners was a reference point to measure the opening diameters. The measured recess volumes were proportional with recess sizes. Recesses with diameters of 7 mm and 11 mm had the smallest and largest cavity volumes of 0.208 mL and 0.521 mL respectively.

3.2. Wettability and surface energy analyses for plasma-treated PET

The surface wettability of untreated and plasma-treated PET recesses is represented by measured WCA in Fig. 3a. The untreated PET surface exhibited a WCA of 77.6 ± 0.6°. The O_2 plasma treatment resulted in a dramatic increase in surface wettability reflected in the decrease of WCA to 46.5 ± 0.5° and 15.3 ± 0.4° for treatment times of 6 s and 18 s respectively. The PET surfaces will be identified by their characteristic WCA due to the consistency in their wettability results. The Fig. 3b illustrates the effect of O_2 plasma treatment on surface energy of PET recesses. The total surface energy of untreated PET was 47.7 ± 0.5 mJ/m^2 with a dispersive component of 44.3 ± 0.7 mJ/m^2 and a polar component of 3.4 ± 0.4 mJ/m^2. The surface energy of plasma-treated PET considerably increased and was proportional with the treatment time. The total surface energy reached 76.5 ± 0.5 mJ/m^2 after O_2 plasma treatment for 18 s. This corresponded to an increase in polar component by a factor of approximately 9 times, while dispersive component showed no significant changes.

3.3. Chemical composition of plasma-treated PET

The chemical composition of untreated PET and plasma-treated PET was characterised through XPS survey spectra as shown in (c) and (d) of the Fig. 3. Both untreated and plasma-treated PET surfaces had distinct peaks for carbon C 1s and oxygen O 1s. Small peak of Si 2p for silicon was also detected as it was potentially originated from the silicon oil used in food packaging production as a de-nesting agent. The wide spectrum of plasma-treated PET surface showed an increase in O 1s peak intensity and decrease in C 1s peak intensity with appearance of additional small peak of nitrogen N 1s. Table 1 presents the O/C ratio and atomic concentration of the elements detected on untreated and plasma-treated PET surfaces. The O/C ratio of untreated PET was 27.07 %

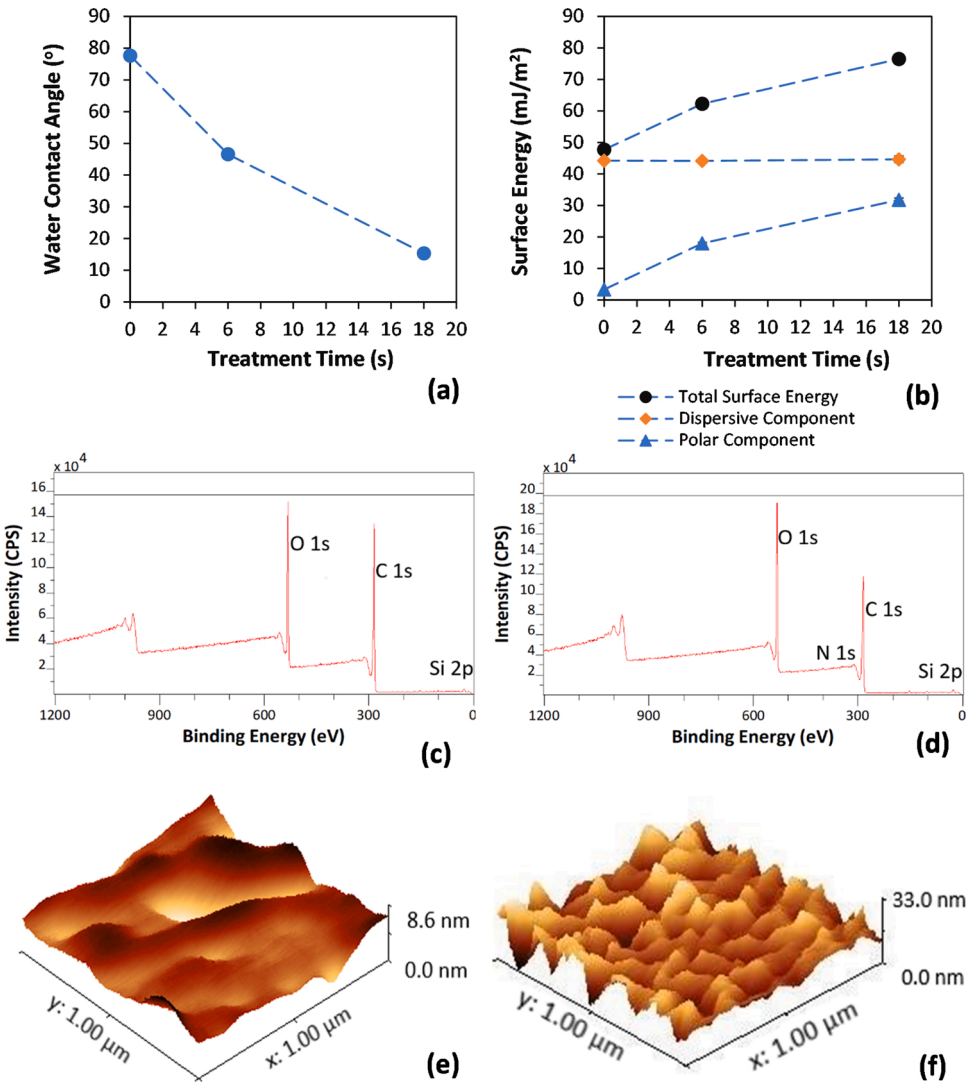

Fig. 3. Changes in surface properties of PET recesses over O_2 plasma treatments; (a) water contact angle, (b) surface energy, (c) wide XPS spectrum of untreated PET, (d) wide XPS spectrum of plasma-treated PET for 18 s, (e) 3D AFM image of untreated PET, (f) 3D AFM image of plasma-treated PET for 18 s.

Table 1
Elemental composition and O/C ratio of PET recess surfaces.

Atomic concentrations of surface elements on the PET surface					
PET Recess Surface	C%	O%	Si%	N%	O/C
Untreated	78.63 ± 0.13	21.28 ± 0.16	0.09 ± 0.06	–	27.07 ± 0.25
Plasma-treated for 6 s	71.17 ± 0.14	28.55 ± 0.12	0.17 ± 0.06	0.11 ± 0.06	40.12 ± 0.21
Plasma-treated for 18 s	69.11 ± 0.36	30.61 ± 0.18	0.08 ± 0.04	0.20 ± 0.13	44.29 ± 0.22

Mean values ± standard deviation (n = 3).

corresponding to O% of 21.28 % and C% of 78.63 %. The O_2 plasma treatment increased O/C ratio to reach 40.12 % and 44.29 % for PET surface treated for 6 s and 18 s respectively. This corresponded to an increase in the oxygen concentration and reduction of carbon concentration as shown in the Table 1. The nitrogen element was present after plasma treatment in small concentrations of 0.11 % and 0.20 % for treatment times of 6 s and 18 s respectively. The C 1s peak was deconvoluted into different components to characterise the functional groups on the PET surface as shown in Fig. S3 in the Supplementary material. The analysed C 1s peak of untreated and plasma-treated PET showed four peak components at binding energies of 285.0, 286.6, 289.0 and 291.5 eV accounting for C—C/C—H, C—O, O—C═O and pi-pi* shake-up bonds respectively. Functional group of C═O bond was formed at a binding energy of 287.5 eV after the plasma treatments. Concentrations of the functional groups are presented in Table S2 in the Supplementary material. The C═O bond was emerged with concentrations of 2.95 % and 5.09 % for plasma treatments of 6 and 18 s respectively.

3.4. Nanoscale surface topography of plasma-treated PET

The surface texture of PET recesses was studied at nanoscale using AFM for scanned areas of 1 µm × 1 µm. The topographical changes before and after plasma treatment were characterised by surface roughness parameters of RMS and Ra as presented in Table S3 in the Supplementary material. The RMS and Ra before plasma treatment were 1.44 nm and 1.12 nm respectively. The PET recesses had rougher surface after 18 s of the plasma treatment attributed to RMS of 6.73 nm and Ra of 4.84 nm. The topological features are visualised in the 3D AFM images for untreated PET (e) and plasma-treated PET (f) in the Fig. 3. The untreated PET had nearly smooth surface, while it showed rougher surface with small spike-like features after the plasma treatment.

3.5. Liquid retention test

3.5.1. Effect of recess size and surface wettability

Retention capacity of PET recess samples (6-recess arrays) of each size (nominal diameter: 7, 8, 9, 9.5, 10, 11 mm) was investigated after mild plasma treatment for 6 s and strong treatment for 18 s. The corresponding surface wettability of the plasma-treated recesses was represented by the characteristic WCA of 46.5° and 15.3° respectively. Fig. 4 shows retention capacity of the recess samples before, after non-localised and localised O_2 plasma treatments of their inner walls. The retention capacity value was average of 6 repeated measurements with simulant liquid (CMC 1 % wt., γ: 52.3 mN/m). The samples with recess diameter of 7 mm maintained full (retention capacity: 1.214 g) before and after localised plasma treatments. The retention capacity of all recesses with diameter > 8 mm decreased with the increase of their sizes. The recess samples treated with localised O_2 plasma exhibited higher retention capacity than untreated samples. The selective improvement in wall surface wettability increased recess capacity to trap the simulant liquid. In contrast, wettability improvement of the combined recess edges and walls (non-localised treatment) diminished their retention capacity to even lower than untreated samples. For example, the retention capacity of untreated sample (recess diameter: 9 mm) increased from 0.696 g to 1.500 g after localised plasma treatment for 18 s. However, the corresponding non-localised plasma decreased the retention capacity to 0.392 g. The retention capacity was proportionate to the wall surface wettability of PET recesses as it was higher for WCA of 15.3° than WCA of 46.5°.

3.5.2. Effect of liquid surface tension and recess surface wettability

Simulant liquids (CMC 1 % wt.) with surface tension values of 72.6, 52.3, 31.5 mN/m were used for retention test of the recess samples. Fig. 5. illustrates the effect of liquid surface tension on retention capacity of untreated samples (a) and samples with localised plasma treatment of 18 s (b). The recess walls treated with O_2 plasma had WCA of 15.3° while the outer edge surface had WCA of 77.6°. For both untreated and plasma-treated samples, the retention capacity was proportionate with the liquid surface tension. For the simulant liquid with surface tension of 72.6 mN/m, the untreated samples maintained full after tilting until recess diameter of 9 mm while plasma-treated samples until recess diameter of 10 mm with retention capacity of 2.594 g. The corresponding untreated sample (recess diameter: 10 mm) had only retention capacity of 0.783 g. The increase in liquid surface tension notably magnified the plasma treatment effect (wall surface wettability) on improving liquid retention of recess samples. Lower surface tension of 52.3 mN/m led to a sharp decrease in retention capacity of untreated recess samples. This had less impact on the retention capacity of the plasma-treated samples as shown in the Fig. 5. However, both untreated and plasma-treated samples for all recess sizes could not retain the lowest surface tension liquid (31.5 mN/m).

3.6. Ageing effect analysis

3.6.1. Ageing effect on surface properties of plasma-treated PET recesses

The surface hydrophobic recovery of plasma-treated PET recesses was investigated for their wettability, surface energy and chemical composition over different ageing times. The recess samples treated with O_2 plasma for 18 s were stored in air. WCA, surface energy and XPS measurements were performed for the aged samples during storage periods of 0, 1, 2, 3, 7, 14, 21, 28, 60 days. Fig. S4 in the Supplementary material shows WCA (a) and surface energy (b) developed on plasma-treated PET over the storage times. The WCA sharply increased from 15.3° to 34.6° in the first three storage days as the ageing rate (degradation rate of surface wettability) of treated PET surface was high. It was then increased gradually to reach 54.8° after 28 days. The WCA was almost stable between 28 and 60 days. The surface energy of plasma-treated PET substantially decreased in the first three days from 76.5 mJ/m^2 to 66.1 mJ/m^2. It then decreased gradually forming a plateau after 28 days. This corresponded to a similar decrease in the polar component of surface energy while the dispersive component was constant. The reduced wettability and surface energy of the aged PET reflected its tendency to return to its original surface properties before the plasma treatment.

The elemental composition of aged PET surface after O_2 plasma treatment showed a decrease in oxygen concentration over the storage periods as shown in Table S4 in the Supplementary material. This revealed a loss of functional polar oxygen groups on the aged PET

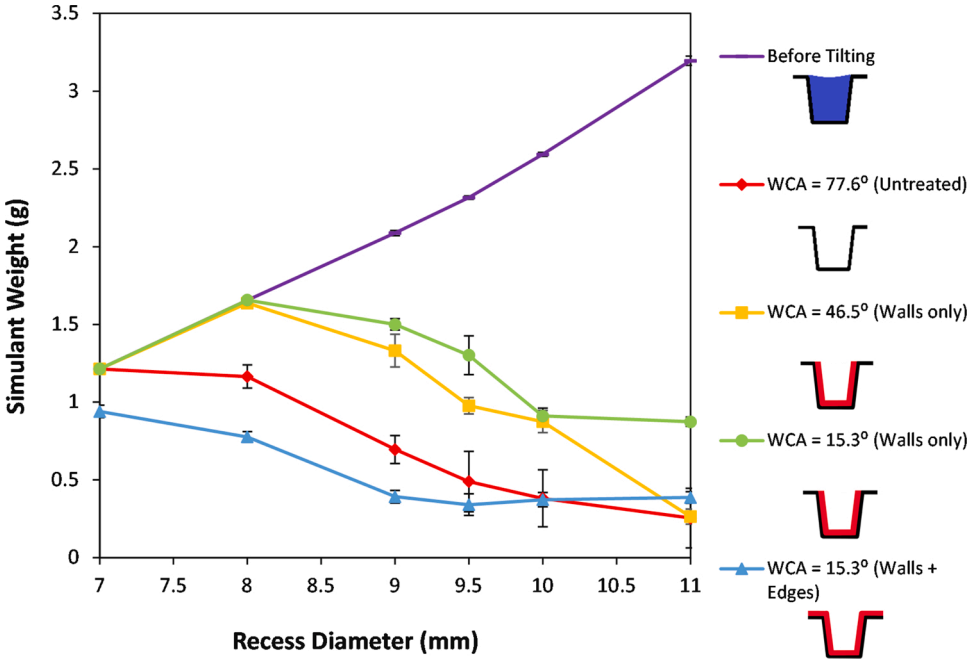

Fig. 4. Retention capacity of tilted PET recess samples (6-recess arrays) with CMC 1 % wt. (γ: 52.3 mN/m) after oxygen plasma treatments; untreated, mild localised treatment (6 s, WCA 46.5°, walls only), strong localised treatment (18 s, WCA 15.3°, walls only), strong full-area treatment (18 s, WCA 15.3°, walls + edges).

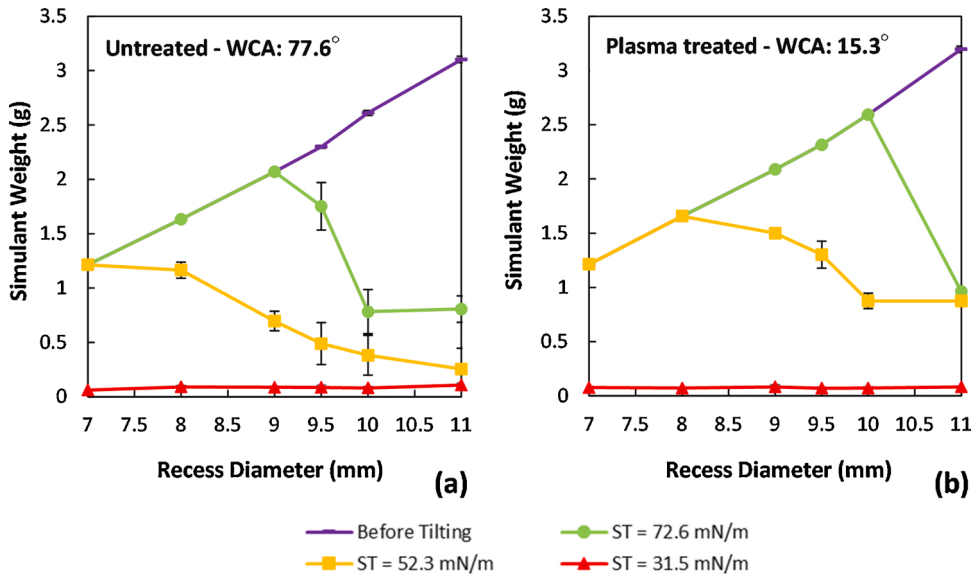

Fig. 5. Retention capacity of PET recess samples (6-recess arrays) with CMC 1 % wt. (γ: 72.6, 52.3, 31.5 mN/m) before (a) and after (b) localised O_2 plasma of internal recess walls.

surface. The highest ageing rate was observed in the first day with a reduction in oxygen concentration from 30.61 % to 28.30 % corresponding to a decrease in O/C ratio from 44.29 % to 39.65 %. The oxygen concentration then slightly decreased over the ageing time. After 60 days, the oxygen concentration was 27.23 % and O/C ratio was 37.90 %, which are still higher than the corresponded values of untreated PET with O% of 21.28 % and O/C of 27.07 %. Therefore, part of oxygen groups introduced by the plasma treatment remains on PET surface for relatively long ageing time. The nitrogen content showed a slight increase over time, while the silicon element showed no significant changes in its concentrations.

3.6.2. Ageing effect on retention capacity of plasma-treated PET recesses

Liquid retention capacity of recess samples after localised O_2 plasma treatment was investigated for storage times of 0, 1, 3, 7, 14, 21, 28, 60 days. This was illustrated in Fig. 6 for samples with recess diameter of 8 mm (a) and 9 mm (b) with simulant liquid (CMC 1 % wt., γ: 52.3 mN/m). The plasma-treated samples with recess diameters of 8 and 9 mm maintained constant retention capacity of 1.664 g and 1.558 g respectively over the storage times. However, the corresponding untreated samples had retention capacity of 1.165 g and 0.696 g respectively as shown in the Fig. 6. For practical application of liquid-holding recesses within food packaging, the retention capacity is also assessed by the liquid volume (mL) retained in a square metre. This capacity can be optimised by hexagonal packing with spacing distance of 1 mm between the circular recesses in 0.9 m^2 taking limited draw ratio of thermoforming process into consideration (Wardhani et al., 2014). Therefore, the retention capacity of plasma-treated recesses with diameter of 8 and 9 mm was 3901 ± 22 and 2972 ± 62 mL/m^2 respectively after 60-day ageing period.

4. Discussion

4.1. Shape profile and dimensions of recesses

The thermoformed PET recesses were dimensionally very consistent and similar to the designed models with only very small deviations as observed in their cross-section visualisation. These deviations may occur due to irregular distribution of wall thickness during vacuum thermoforming with high draw ratios. The elastic shrinkage and release of stress residuals of the formed PET recesses can also contribute to these small scale dimensional deviations (Ashter, 2014; Morye, 2005; Throne,

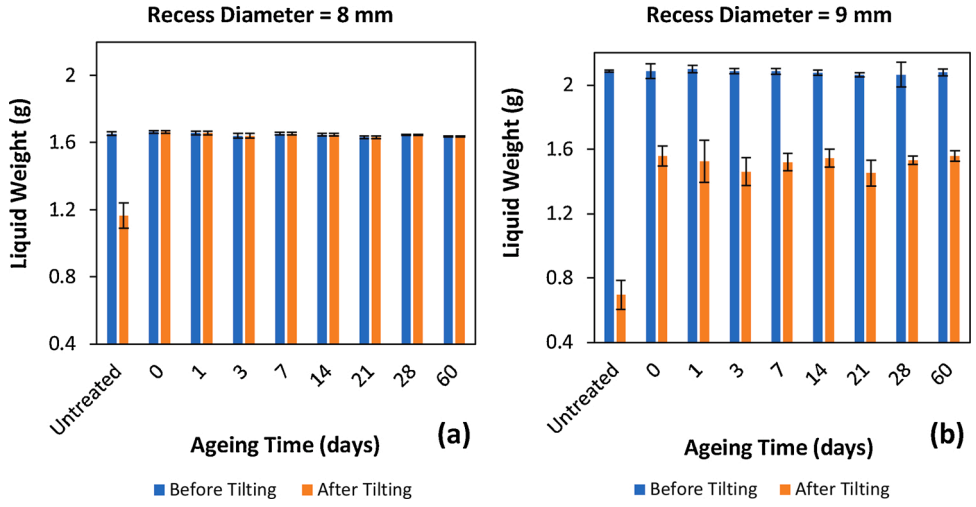

Fig. 6. Liquid retention capacity of plasma-treated PET samples with nominal recess diameters of 8 mm (a) and 9 mm (b) over different storage times.

2017).

4.2. Plasma impact on recess surface properties

The O_2 plasma treatment of PET recesses increased their surface hydrophilicity and therefore their wettability for water-based liquids (Karbowiak et al., 2006; Shenton & Stevens, 2001; Vesel & Mozetic, 2017). It functionalised the untreated PET surface with hydrophilic oxygen groups, such as C—OH and COOH causing a decrease in WCA. The prolonged plasma treatment further decreased the WCA to 15.3° as more hydrophilic groups were attached on the treated surface (Junkar et al., 2009; Vesel et al., 2008). The modification treatment is initiated with scission of C—C bonds in the polymer chains and hydrogen abstraction. This is carried out by the highly reactive plasma species, such as radical oxygen and hydroxyl groups forming radical sites. The excited oxygen in plasma glow reacts with the radical sites to generate different oxygen groups including C—OH, C═O and COOH (Vesel & Mozetic, 2017; Yang et al., 2009). A comparable decrease in WCA from 72° to 19° on PET surface was found after O_2 plasma in work of Junkar et al. (2009). The polar oxygen groups also contributed to the substantial increase in polar component of surface energy by 28.5 mJ/m^2 (3.4–31.9 mJ/m^2), which primarily accounted for the increase in total surface energy of 28.8 mJ/m^2. A comparable increase in surface energy of plasma-treated PET was found by Yang et al. (2009).

Oxygen plasma treatment resulted in increasing oxygen concentration and hence O/C (Junkar et al., 2009; Vesel & Mozetic, 2017). This was manifested as additional oxygen groups, such as C═O were introduced to the treated recess surface (Yang et al., 2009). The O/C was also proportionate with treatment time as high number of active sites are ready to incorporate oxygen groups for prolonged treatments (Vesel et al., 2008). Therefore, the increase in oxygen concentration can explain the increased wettability and surface energy of the plasma-treated PET. Similar effects of plasma treatments have been reported by different studies (Homola et al., 2012; Junkar et al., 2009; Yang et al., 2009). The C 1s peak analysis (Table S2, Supplementary material) showed that under the plasma treatment new C═O was formed, while absent from the untreated samples. This has been observed to significantly improve the surface polarity and wettability in literature (Lv et al., 2016; Vesel et al., 2008). As well as an increase in oxygen to carbon ratio, small amounts of nitrogen were detected in the plasma-treated samples. This element might be present due to post-plasma reaction between the activated surface and the nitrogen in air (Xie et al., 2012). The peak of pi-pi satellite appeared due to the emitted photoelectrons of excited aromatic phenyl groups (Dowling et al., 2012).

Etching effect of the plasma treatment led a substantial increase in nanoscale surface roughness of the PET recesses. The excited plasma particles have more predominating etching and eroding impact on the amorphous areas of the PET surface than crystalline areas. The varied etching rate over the treated surface may have resulted in rougher PET surface with larger projected area (Kostov et al., 2010). This could contribute to long-lasting improvement in wettability of PET recesses even after ageing due to increased interface between the PET surface and contacting liquid (Kostov et al., 2010; Nosonovsky & Bhushan, 2005), based on Wenzel law (Wenzel, 1936).

4.3. Liquid retention capacity of PET recesses

The localised increase in wettability and surface energy was an effective means of enhancing liquid retention of the PET recesses. This allows manufacturing of food plastic trays incorporated with recesses of increased liquid-holding capacity. Therefore, food exudate released from even very exudative food products can be isolated and retained in the designated recesses during the product shelf life. The liquid trapping functionality gained by the capillary recesses can be explained by the liquid pinning phenomenon and pressures acting on liquid interface. This was investigated by (Extrand, 2017, 2018a) for capillary tubes and orifices in vertical and inclined positions. Liquid in a capillarity with closed-top end is subject to encountering atmospheric and hydrostatic pressures. A capillary pressure also acts on the liquid to form a meniscus on the recess walls (Extrand, 2017). Liquid drainage in a tilted large capillarity such a recess is induced by propagation of air finger (Taylor finger) into the liquid-air interface due to instability in the liquid meniscus. This results in replacing the liquid with air as the liquid forms a film on the capillarity walls and drains out of the open end (Davies & Taylor, 1950; Kumar et al., 2018). The recess opening has a geometrical valving functionality where the capillary pressure induces liquid pinning effects and forms valving pressure barrier (Wang et al., 2013). This enhances stability of the liquid menisci and prevent liquid drainage due to phenomenon of Taylor finger (Kumar et al., 2018). This was manifested in stable menisci on recess openings of small sizes as the capillary pressure and pinning effects are large enough to restrict initiation of the air finger. The atmospheric pressure upwardly acting on liquid meniscus, therefore, was able to retain the liquid in the tilted small recesses as explained by Extrand (2017). For example, the recesses with diameter of 7 mm were maintained full during and after tilting even without plasma treatment. However, the liquid interface had smaller curvature for untreated recesses with larger sizes as the capillary pressure decreased (Extrand, 2017). The recess inclination during tilting resulted in local change in the hydrostatic pressure acting on the liquid interface (Extrand, 2018b). This resulted in liquid advancing on one recess wall and receding on the other wall as described by work of Extrand (2018a). The low capillary pressure of untreated large recesses resulted in unstable meniscus and diminished pining effect against the advanced meniscus. This facilitated air finger propagation leading to liquid drainage of the recesses (Extrand, 2017, 2018a; Kumar et al., 2018).

On the other hand, the localised plasma treatment of internal recess walls improved the pinning effect and pressure barrier on the recess opening. The low surface energy of PET recesses allowed localised plasma treatment to induce a considerable variation in wetting properties between the inner walls and outer edges of the treated recesses (Awaja et al., 2009). This introduced additional pinning effect due to the wettability variation, which acts as capillary burst valve. Therefore, the recess openings gained improved liquid pinning from combined valving effects of geometrical and wettability changes (Cho et al., 2007; Feng et al., 2003). This provided the liquid menisci with more resistance to the air finger propagation and liquid drainage, particularly for larger recesses in comparison with corresponding untreated recesses. Consequently, the stability of liquid menisci and pinning effects were enhanced for the plasma-treated recesses leading to higher liquid retention capacity. The retention capacity was also proportionate with wall surface wettability as the wetting properties between the walls and outer edges were further magnified (Andersson et al., 2001; Cho et al., 2007; Extrand, 2017). However, the decrease in liquid surface tension resulted in less stable liquid interfaces and lower capillary pressure barriers. Therefore, the recess resistance to drainage was undermined causing reduced retention capacity. This was also found by Kumar et al. (2018) in liquid drainage from closed tubes. For liquid with the lowest surface tension (31.5 mN/m), there was a lack of retention capacity as the liquid surface tension was lower than the surface energy of the untreated substrate (47.7 mJ/m^2). This caused a complete wetting of the recess edges leading to evacuation of the liquid from recess cavities in all conditions (both untreated and locally treated). Non-localised plasma treatment increased hydrophilicity (WCA: 15.3°) on both wall and edge surfaces. The highly hydrophilic outer edges led to enhancing adhesive forces on the edges surface. These forces compete with cohesive forces of the liquid and prevent pinning of liquid menisci. This was reported by Kazemzadeh et al. (2013) for highly hydrophilic capillary valves. The retention capacity of samples (recess diameter: 9 mm) with localised and non-localised O_2 plasma treatment (WCA: 15.3°) was 1.500 g and 0.392 g respectively, but retention capacity of the corresponding untreated

samples was 0.696 g. This concludes that the liquid retention improvement requires a distinct difference in wetting characteristics between the recess walls and their outer edges.

4.4. Longevity and practicality of plasma treatment

The improved retention capacity and surface properties of PET recesses gained by the O_2 plasma treatment were subject to ageing during the storage periods. This was manifested in increasing WCA and decreasing surface energy over 60 days. It also corresponded to the decrease in oxygen concentration and O/C ratio over the ageing time. Ageing phenomenon is observed in polymer surfaces after plasma treatments as the aged surfaces exhibit tendency to lose their polar groups and become more hydrophobic surfaces (Vesel et al., 2008). This includes migration of non-polar groups from the polymer matrix to the treated surface. The polymer chains may also experience reorientation resulting in burying the functional groups inside deeper layers of the polymer surface (Kostov et al., 2010; Pankaj et al., 2014). However, WCA on the aged PET after 60 days was still substantially lower than untreated PET (53.7° vs 77.6°), and surface energy remained higher than the untreated PET (see Fig. S4). This suggests that plasma treatment induced a permanent increase in the surface wettability and energy (Homola et al., 2012). A comparable recovery behaviour was reported by Kostov et al. (2010) and Homola et al. (2012). Despite the apparent reduction in surface wettability and oxygen to carbon ratio, the partial hydrophobic recovery still allowed the wettability transition between the recess walls and outer edges to be maintained. This contributed to improved pinning effect and retention capacity of the treated recesses during ageing times (Andersson et al., 2001). Even after 60 days, the treated recess cavity was fully functional, allowing similar high retention, with no drop in performance. For liquids with comparable surface tension value of meat exudate, retention capacity of aged PET recesses with diameter of 9 mm was 2972 ± 62 mL/m^2 as increased by 2.24 times after the localised plasma treatment. This showed a comparable retention capacity with conventional absorbent meat pads. These absorbent pads are typically used in meat packaging industry with retention capacity of 3000 mL/m^2 (2949 mL/m^2 as assessed in laboratory by simulant liquid on a sample). The enhanced liquid retention lasts long enough for practical use by packaging companies, and realistically a plasma unit could easily be incorporated to the production line (Van Deynse et al., 2015). This can lead to promising meat packaging capable to take away the need for conventional absorbent pads, easier to recycle and maybe for the consumer to handle.

5. Conclusions

This work has demonstrated that localised increases in surface wettability of capillary recess walls by plasma treatment is an effective method to increase their liquid retention capacity. Plasma-treated PET recesses of extended sizes demonstrated a considerable and long-lasting increase in their liquid retention capacity when compared with untreated PET samples. The localised oxygen plasma treatment introduced polar oxygen groups onto the PET recess surface resulting in an increase in surface wettability and energy. These surface energy increases were partially diminished over time due to ageing effects. However, this was not at the expense of liquid retention capacity as the plasma-treated inner walls maintained wetting characteristics different to the untreated outer edges. The treated recesses were able to exploit the capillary valving functionalities, even after 60 days of ageing, to form more stable menisci and prevent liquid drainage. This demonstrated the viability of using plasma treatment in food packaging to effectively isolate any excessive exudate. The plasma treatment can be scaled up to be a continuous treatment process for food packaging by using atmospheric plasma technology. These food trays can be manufactured from fully recyclable materials, such as PET, PE and PP ensuring more recyclable packaging trays with greater environmental footprint. The capillary recesses can also be easily cleaned after use to facilitate the recycling process. This will allow millions of food trays to be recycled and support packaging sustainability. Further, absorbent pads used in food packaging will be avoided, which primarily end up in landfill placing additional environmental burden. While the approach is focussed on application for meat exudate it is equally transferable to other food products such as soft fruits. Potential utilisation of this technique with bio-derived plastics in place of PET can lead to further sustainability improvements.

CRediT authorship contribution statement

Alaa Alaizoki: Investigation, Conceptualization, Methodology, Writing – original draft, Visualization. **Christopher Phillips:** Supervision, Writing – review & editing, Validation. **David Parker:** Resources, Supervision, Project administration. **Craig Hardwick:** Supervision. **Chris Griffiths:** Resources. **Davide Deganello:** Conceptualization, Supervision, Methodology, Writing – review & editing, Validation, Project administration.

Declaration of Competing Interest

Authors declare that a patent (Application number: GB2019580.6) has applied in relation to this work.

Acknowledgements

This work was financially supported by Materials and Manufacturing Academy (M2A) through funding from the European Social Fund via the Welsh Government (c80816), the Engineering and Physical Sciences Research Council (Grant Ref: EP/L015099/1) and Klockner Pentaplast Group. Furthermore, the authors would like to acknowledge the assistance provided by Swansea University, College of Engineering AIM Facility, which was funded in part by the EPSRC (EP/M028267/1), the European Regional Development Fund through the Welsh Government (80708) and the Ser Solar project via Welsh Government. The authors thank James McGettrick for the assistance in XPS analysis.

Appendix A. Supplementary data

Supplementary material related to this article can be found, in the online version, at doi:https://doi.org/10.1016/j.fpsl.2021.100759.

References

Andersson, H., Van der Wijngaart, W., Griss, P., Niklaus, F., & Stemme, G. (2001). Hydrophobic valves of plasma deposited octafluorocyclobutane in DRIE channels. *Sensors and Actuators, B: Chemical, 75*(1–2), 136–141. https://doi.org/10.1016/S0925-4005(00)00675-4

Ashter, S. A. (2014). The thermoforming process. *Thermoforming of single and multilayer laminates* (pp. 13–38). https://doi.org/10.1016/b978-1-4557-3172-5.00002-5

Awaja, F., Gilbert, M., Kelly, G., Fox, B., & Pigram, P. J. (2009). Adhesion of polymers. *Progress in Polymer Science (Oxford), 34*(9), 948–968. https://doi.org/10.1016/j.progpolymsci.2009.04.007

Baldwin, A. F., Bliton, R. J., Brown, J. Z., & Dorsey, K. D. (2007). Absorbent mats for food packaging (Patent No. US7306094). United States. https://patents.google.com/patent/US7306094B2/en?oq=US7306094.

Berry, J. D., Neeson, M. J., Dagastine, R. R., Chan, D. Y. C., & Tabor, R. F. (2015). Measurement of surface and interfacial tension using pendant drop tensiometry. *Journal of Colloid and Interface Science, 454*, 226–237. https://doi.org/10.1016/j.jcis.2015.05.012

Biji, K. B., Ravishankar, C. N., Mohan, C. O., & Srinivasa Gopal, T. K. (2015). Smart packaging systems for food applications: A review. *Journal of Food Science and Technology, 52*(10), 6125–6135. https://doi.org/10.1007/s13197-015-1766-7

Buntinx, M., Willems, G., Knockaert, G., Adons, D., Yperman, J., Carleer, R., & Peeters, R. (2014). Evaluation of the thickness and oxygen transmission rate before and after thermoforming mono- and multi-layer sheets into trays with variable depth. *Polymers, 6*(12), 3019–3043. https://doi.org/10.3390/polym6123019

Carey, T., Jones, C., Le Moal, F., Deganello, D., & Torrisi, F. (2018). Spray-coating thin films on three-dimensional surfaces for a semitransparent capacitive-touch device. *ACS Applied Materials and Interfaces, 10*(23), 19948–19956. https://doi.org/10.1021/acsami.8b02784

Cho, H., Kim, H. Y., Kang, J. Y., & Kim, T. S. (2007). How the capillary burst microvalve works. *Journal of Colloid and Interface Science, 306*(2), 379–385. https://doi.org/10.1016/j.jcis.2006.10.077

Davidson, R. P., Becke, G. S., & Minnett, J. C. (2013). Food tray with integrated liquid-retention system (Patent No. US8596490). United States. https://patents.google.com/patent/US8596490B2/en?q=Food+tray+integrated+liquid-fangretention+system&oq=Food+tray+with+integrated+liquid-retention+system.

Davies, R. M., & Taylor, G. (1950). The mechanics of large bubbles rising through extended liquids and through liquids in tubes. *Proceedings of the Royal Society of London. Series A, Mathematical and Physical Sciences, 200*(1062), 375–390. http://www.jstor.org/stable/98449.

Den Hertog-Meischke, M. J. A., Smulders, F. J. M., & Van Logtestijn, J. G. (1998). The effect of storage temperature on drip loss from fresh beef. *Journal of the Science of Food and Agriculture, 78*(4), 522–526. https://doi.org/10.1002/(SICI)1097-0010(199812)78:4<522::AID-JSFA150>3.0.CO;2-F

Dowling, D. P., Tynan, J., Ward, P., Hynes, A. M., Cullen, J., & Byrne, G. (2012). Atmospheric pressure plasma treatment of amorphous polyethylene terephthalate for enhanced heatsealing properties. *International Journal of Adhesion and Adhesives, 35*, 1–8. https://doi.org/10.1016/j.ijadhadh.2012.01.025

Durdag, K., Pendleton, B., Hamlyn, R., Gunn, V., & Etchells, M. (2014). Biodegradable polymer non-woven absorbent pad with absorbency and antimicrobial chemistry (Patent No. US 8828516). United States. https://patents.google.com/patent/US8828516B2/en.

Erdogan, E. S., & Eksi, O. (2014). Prediction of wall thickness distribution in simple thermoforming moulds. *Strojniški Vestnik – Journal of Mechanical Engineering, 60*(3), 195–202. https://doi.org/10.5545/sv-jme.2013.1486

Extrand, C. W. (2017). Spontaneous draining of liquids from vertically oriented tubes. *Langmuir, 33*(45), 12903–12907. https://doi.org/10.1021/acs.langmuir.7b03247

Extrand, C. W. (2018a). Drainage from a fluid-handling component because of inclination. *Langmuir, 34*(1), 126–130. https://doi.org/10.1021/acs.langmuir.7b03791

Extrand, C. W. (2018b). Drainage from a fluid-handling component with multiple orifices due to inclination or rotation. *Langmuir, 34*(14), 4159–4165. https://doi.org/10.1021/acs.langmuir.7b04271

Farouk, M. M., Mustafa, N. M., Wu, G., & Krsinic, G. (2012). The "sponge effect" hypothesis: An alternative explanation of the improvement in the waterholding capacity of meat with ageing. *Meat Science, 90*(3), 670–677. https://doi.org/10.1016/j.meatsci.2011.10.012

Feng, Y., Zhou, Z., Ye, X., & Xiong, J. (2003). Passive valves based on hydrophobic microfluidics. *Sensors and Actuators, A: Physical, 108*(1–3), 138–143. https://doi.org/10.1016/S0924-4247(03)00363-7

Gaikwad, K. K., Singh, S., & Ajji, A. (2019). Moisture absorbers for food packaging applications. *Environmental Chemistry Letters, 17*(2), 609–628. https://doi.org/10.1007/s10311-018-0810-z

Gouvêa, D. M., Mendonça, R. C. S., Lopez, M. E. S., & Batalha, L. S. (2016). Absorbent food pads containing bacteriophages for potential antimicrobial use in refrigerated food products. *LWT - Food Science and Technology, 67*, 159–166. https://doi.org/10.1016/j.lwt.2015.11.043

Guo, Z., Zhang, J., Zhang, T., Li, C., Zhang, Y., & Bai, J. (2012). Liquid viscosities, excess properties, and viscous flow thermodynamics of triethylene glycol + water mixtures at T = (298.15, 303.15, 308.15, 313.15, and 318.15) K. *Journal of Molecular Liquids, 165*, 27–31. https://doi.org/10.1016/j.molliq.2011.10.003

Han, B.-S. (2009). Absorbent and Antibacterial Polystyrene Paper (PSP) Sheet, Method for Producing Thereof and Tray using The Same (Patent No. US 2009/0093559). United States. https://patents.google.com/patent/US20090093559.

Homola, T., Matoušek, J., Hergelová, B., Kormunda, M., Wu, L. Y. L., & Černák, M. (2012). Activation of poly(ethylene terephthalate) surfaces by atmospheric pressure plasma. *Polymer Degradation and Stability, 97*(11), 2249–2254. https://doi.org/10.1016/j.polymdegradstab.2012.08.001

Huff-Lonergan, E., & Lonergan, S. M. (2005). Mechanisms of water-holding capacity of meat: The role of postmortem biochemical and structural changes. *Meat Science, 71*(1), 194–204. https://doi.org/10.1016/j.meatsci.2005.04.022

Jensen, R., & Versteylen, S. (2008). Consumer food storage package with absorbent food pad (Patent No. US 2008/019957). United States. moz-extension://17abc4bf-e19e-4e55-a407-ac25b3c3f5d7/enhanced-reader.html?openApp&pdf=https%3A%2F%2Fpatentimages.storage.googleapis.com%2F80%2F59%2Fde%2F5d29266a443359%2FUS20080199577A1.pdf.

Jucius, D., Kopustinskas, V., Grigaliunas, V., Guobiene, A., Lazauskas, A., & Andrulevičius, M. (2015). Highly hydrophilic poly(ethylene terephthalate) films prepared by combined hot embossing and plasma treatment techniques. *Applied Surface Science, 349*, 200–210. https://doi.org/10.1016/j.apsusc.2015.04.221

Junkar, I., Vesel, A., Cvelbar, U., Mozetič, M., & Strnad, S. (2009). Influence of oxygen and nitrogen plasma treatment on polyethylene terephthalate (PET) polymers. *Vacuum, 84*(1), 83–85. https://doi.org/10.1016/j.vacuum.2009.04.011

Karbowiak, T., Debeaufort, F., & Voilley, A. (2006). Importance of surface tension characterization for food, pharmaceutical and packaging products: A review. *Critical Reviews in Food Science and Nutrition, 46*(5), 391–407. https://doi.org/10.1080/10408390591000884

Kazemzadeh, A., Ganesan, P., Ibrahim, F., He, S., & Madou, M. J. (2013). The effect of contact angles and capillary dimensions on the burst frequency of super hydrophilic and hydrophilic centrifugal microfluidic platforms, a CFD study. *PLoS One, 8*(9), Article e73002. https://doi.org/10.1371/journal.pone.0073002

Kim, G. D., Jung, E. Y., Lim, H. J., Yang, H. S., Joo, S. T., & Jeong, J. Y. (2013). Influence of meat exudates on the quality characteristics of fresh and freeze-thawed pork. *Meat Science, 95*(2), 323–329. https://doi.org/10.1016/j.meatsci.2013.05.007

Klimovič, M., & Pekař, M. (2007). Untypical rheological behaviour of the lignite-carboxymethylcellulose-water dispersion system. *Colloid and Polymer Science, 285*(8), 865–872. https://doi.org/10.1007/s00396-006-1632-2

Kostov, K. G., dos Santos, A. L. R., Honda, R. Y., Nascente, P. A. P., Kayama, M. E., Algatti, M. A., & Mota, R. P. (2010). Treatment of PET and PU polymers by atmospheric pressure plasma generated in dielectric barrier discharge in air. *Surface and Coatings Technology, 204*(18–19), 3064–3068. https://doi.org/10.1016/j.surfcoat.2010.02.008

Kumar, A., Ray, S., & Das, G. (2018). Draining phenomenon in closed narrow tubes pierced at the top: An experimental and theoretical analysis. *Scientific Reports, 8*(1), 14114. https://doi.org/10.1038/s41598-018-32359-5

LaRue, J. M., Cappel, C. E., & Petlak, F. A. (2011). Container having internal reservoir (Patent No. US7921992). United States. https://patents.google.com/patent/US7921992B2/en?oq=+7921992.

Lee, K. T. (2010). Quality and safety aspects of meat products as affected by various physical manipulations of packaging materials. *Meat Science, 86*(1), 138–150. https://doi.org/10.1016/j.meatsci.2010.04.035

Lee, K. T., Goddard, J. M., & Hotchkiss, J. H. (2009). Plasma modification of polyolefin surfaces. *Packaging Technology and Science, 22*(3), 139–150. https://doi.org/10.1002/pts.829

Leite, W. O., Campos Rubio, J. C., Mata, F., Hanafi, I., & Carrasco, A. (2018). Dimensional and geometrical errors in vacuum thermoforming products: An approach to modeling and optimization by multiple response optimization. *Measurement Science Review, 18*(3), 113–122. https://doi.org/10.1515/msr-2018-0017

Licciardello, F. (2017). Packaging, blessing in disguise. Review on its diverse contribution to food sustainability. *Trends in Food Science and Technology, 65*, 32–39. https://doi.org/10.1016/j.tifs.2017.05.003

Lu, G., Wang, X. D., & Duan, Y. Y. (2013). Study on initial stage of capillary rise dynamics. *Colloids and Surfaces A: Physicochemical and Engineering Aspects, 433*, 95–103. https://doi.org/10.1016/j.colsurfa.2013.05.004

Lv, J., Zhou, Q., Zhi, T., Gao, D., & Wang, C. (2016). Environmentally friendly surface modification of polyethylene terephthalate (PET) fabric by low-temperature oxygen plasma and carboxymethyl chitosan. *Journal of Cleaner Production, 118*, 187–196. https://doi.org/10.1016/J.JCLEPRO.2016.01.058

Maga, D., Hiebel, M., & Aryan, V. (2019). *A comparative life cycle assessment of meat trays made of various packaging materials*. https://doi.org/10.3390/su11195324

Miehle, E., Bader-Mittermaier, S., Schweiggert-Weisz, U., Hauner, H., & Eisner, P. (2021). Effect of physicochemical properties of carboxymethyl cellulose on diffusion of glucose. *Nutrients, 13*(5). https://doi.org/10.3390/nu13051398

Morye, S. S. (2005). A comparison of the thermoformability of a PPE/PP blend with thermoformable ABS. Part I: Small deformation methods. *Polymer Engineering & Science, 45*(10), 1369–1376. https://doi.org/10.1002/pen.20416

Nisticò, R. (2020). Polyethylene terephthalate (PET) in the packaging industry. *Polymer Testing, 90*, Article 106707. https://doi.org/10.1016/j.polymertesting.2020.106707

Nosonovsky, M., & Bhushan, B. (2005). Roughness optimization for biomimetic superhydrophobic surfaces. *Microsystem Technologies, 11*(7), 535–549. https://doi.org/10.1007/s00542-005-0602-9

Otoni, C. G., Espitia, P. J. P., Avena-Bustillos, R. J., & McHugh, T. H. (2016). Trends in antimicrobial food packaging systems: Emitting sachets and absorbent pads. *Food Research International, 83*, 60–73. https://doi.org/10.1016/j.foodres.2016.02.018

Pandiyaraj, K. N., Selvarajan, V., Deshmukh, R. R., Yoganand, P., Balasubramanian, S., & Maruthamuthu, S. (2013). Low pressure DC glow discharge air plasma surface treatment of polyethylene (PE) film for improvement of adhesive properties. *Plasma Science and Technology, 15*(1), 56. https://doi.org/10.1088/1009-0630/15/1/10

Pankaj, S. K., Bueno-Ferrer, C., Misra, N. N., Milosavljević, V., O'Donnell, C. P., Bourke, P., Keener, K. M., & Cullen, P. J. (2014). Applications of cold plasma technology in food packaging. *Trends in Food Science and Technology, 35*(1), 5–17. https://doi.org/10.1016/j.tifs.2013.10.009

Realini, C. E., & Marcos, B. (2014). Active and intelligent packaging systems for a modern society. *Meat Science, 98*(3), 404–419. https://doi.org/10.1016/j.meatsci.2014.06.031

Sahin, S., & Sumnu, S. G. (2007). Size, shape, volume, and related physical attributes. *Physical properties of foods* (pp. 1–37). New York: Springer. https://doi.org/10.1007/0-387-30808-3_1

Schmidt, A. (2013). Absorbent insert for foodstuff packaging (Patent No. US8414997). United States. https://patents.google.com/patent/US8414997B2/en?oq=US+8.414%2C997+B2.

Shenton, M. J., & Stevens, G. C. (2001). Surface modification of polymer surfaces: Atmospheric plasma versus vacuum plasma treatments. *Journal of Physics D: Applied Physics, 34*(18), 2761–2768. https://doi.org/10.1088/0022-3727/34/18/308

Si, Y., Yu, C., Dong, Z., & Jiang, L. (2018). Wetting and spreading: Fundamental theories to cutting-edge applications. *Current Opinion in Colloid and Interface Science, 36*, 10–19. https://doi.org/10.1016/j.cocis.2017.12.006

Throne, J. (2017). Thermoforming. *Applied plastics engineering handbook: Processing, materials, and applications* (2nd ed., pp. 345–375). Elsevier Inc.. https://doi.org/10.1016/B978-0-323-39040-8.00016-X

Ursu, A. V., Marcati, A., Michaud, P., & Djelveh, G. (2016). Valorisation of industrial cooked ham by-products as functional ingredients. *Journal of Food Engineering, 190*, 54–60. https://doi.org/10.1016/j.jfoodeng.2016.06.013

Van Deynse, A., Cools, P., Leys, C., De Geyter, N., & Morent, R. (2015). Surface activation of polyethylene with an argon atmospheric pressure plasma jet: Influence of applied power and flow rate. *Applied Surface Science, 328*, 269–278. https://doi.org/10.1016/j.apsusc.2014.12.075

Vesel, A., & Mozetic, M. (2017). New developments in surface functionalization of polymers using controlled plasma treatments. *Journal of Physics D: Applied Physics, 50* (29), Article 293001. https://doi.org/10.1088/1361-6463/AA748A

Vesel, A., Junkar, I., Cvelbar, U., Kovac, J., & Mozetic, M. (2008). Surface modification of polyester by oxygen- and nitrogen-plasma treatment. *Surface and Interface Analysis, 40*(11), 1444–1453. https://doi.org/10.1002/sia.2923

Wang, Z., Yen, H. Y., Chang, C. C., Sheng, Y. J., & Tsao, H. K. (2013). Trapped liquid drop at the end of capillary. *Langmuir, 29*(39), 12154–12161. https://doi.org/10.1021/la4026602

Wardhani, R., Putu, S., Sanjoto, B. L., Nur, H., & Hari, S. (2014). Numerical simulation of multipoint forming with circular die pins in hexagonal packing. *Applied Mechanics and Materials, 493*, 589–593. https://doi.org/10.4028/www.scientific.net/AMM.493.589

Warner, R. D. (2017). The eating quality of meat-IV water-holding capacity and juiciness. *Lawrie's meat science* (8th ed., pp. 419–459). Elsevier. https://doi.org/10.1016/B978-0-08-100694-8.00014-5

Wenzel, R. N. (1936). Resistance of solid surfaces to wetting by water. *Industrial and Engineering Chemistry, 28*(8), 988–994. https://doi.org/10.1021/ie50320a024

Xie, L., Dai, Q., Du, G., Deng, Q., & Liu, G. (2012). Study on surface modification of polyethylene terephthalate(PET) film by RF-Ar/O 2 plasma treatment. *Applied Mechanics and Materials, 200*, 94–98. https://doi.org/10.4028/www.scientific.net/AMM.200.194

Yang, L., Chen, J., Guo, Y., & Zhang, Z. (2009). Surface modification of a biomedical polyethylene terephthalate (PET) by air plasma. *Applied Surface Science, 255*(8), 4446–4451. https://doi.org/10.1016/j.apsusc.2008.11.048

Zille, A., Oliveira, F. R., & Souto, P. A. P. (2015). Plasma treatment in textile industry. *Plasma Processes and Polymers, 12*(2), 98–131. https://doi.org/10.1002/ppap.201400052

Zimmermann, M., Hunziker, P., & Delamarche, E. (2008). Valves for autonomous capillary systems. *Microfluidics and Nanofluidics, 5*(3), 395–402. https://doi.org/10.1007/s10404-007-0256-2